# Modelling of aerodynamic rotor interaction for multi-rotor wind turbines

Mads Christian Baungaard

July 15th, 2019

Supervisors:
Paul van der Laan (DTU Wind Energy)
Mikkel Kiilerich Østerlund (Vestas)

**DTU Wind Energy**
Department of Wind Energy

# Introduction

# Vestas 4R-V29

- Installed at Risø in April 2016 and decomissioned in December 2018
- Consists of four V29-225 kW rotors
- Rotor interaction was found to increase power by $\approx 2\%$ and to enhance the wake recovery, van der Laan et. al (2019).

# Multi-rotor wind turbines 1900-1950

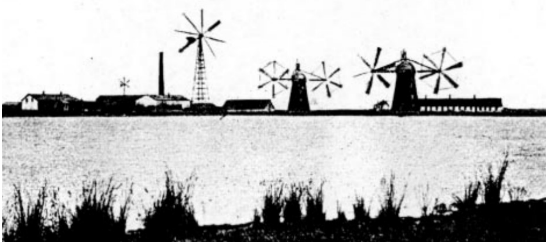

Saltbæk Vig, 1900-1910

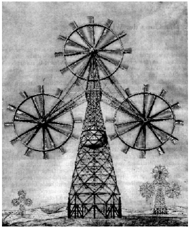

Honnef's "Kraftwerke", 1932

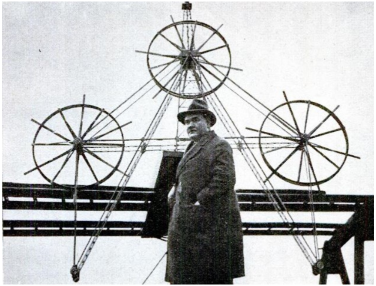

Honnef's "Kraftwerke" prototype, 1932-1939

Mathiasberg, 1940-1945

# Multi-rotor wind turbines 1950-2000

- First systematic tests in wind tunnel by Smulders et. al (1984) with three main results:
  1. Rotor interaction increases average power production
  2. Effect is negligible for $s_h/D \geq 0.4$
  3. Self-aligning moment, when yawed

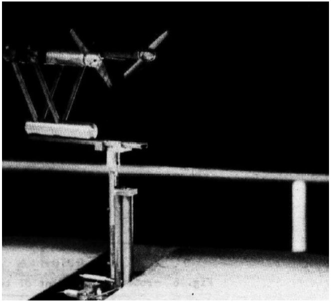

Smulders et al., 1984

Karl van der Linden, 1984

Largerwey, 1986

# Intermezzo: Why multi-rotor wind turbines?

- Galilei 1638: $A \sim L^2$ and $V \sim L^3$
- Jamieson 1995: Advantage for multi-rotor wind turbines

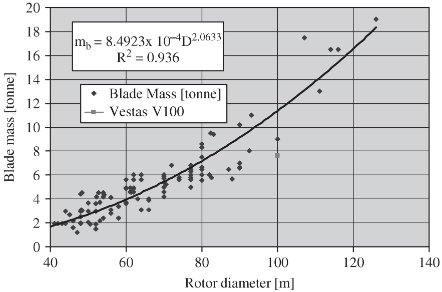


$$M(D) = \alpha D^{\beta}$$

| Model | D [m] | M [ton] |
|---|---|---|
| Siemens 3 MW | 108 | 133 |
| Siemens 6 MW | 154 | 350 |

$\Rightarrow \beta \approx 2.7$

$$N \cdot (\pi D^2) = \pi D^2_{eq,single}$$

$$\frac{M_{multi}}{M_{eq,single}} = \frac{N \alpha D^{\beta}}{\alpha D^{\beta}_{eq,single}} = N^{-\beta/2+1}$$

For $N=4$: $\frac{M_{multi}}{M_{eq,single}} = 0.62$

# Intermezzo: Why multi-rotor wind turbines?

- Galilei 1638: $A \sim L^2$ and $V \sim L^3$
- Jamieson 1995: Advantage for multi-rotor wind turbines

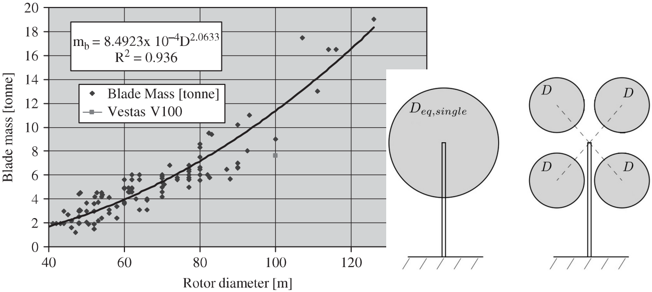


$$M(D) = \alpha D^{\beta}$$

| Model | D [m] | M [ton] |
|---|---|---|
| Siemens 3 MW | 108 | 133 |
| Siemens 6 MW | 154 | 350 |

$\Rightarrow \beta \approx 2.7$

$$\boxed{N \cdot (\pi D^2) = \pi D^2_{eq,single}}$$

$$\frac{M_{multi}}{M_{eq,single}} = \frac{N \alpha D^{\beta}}{\alpha D^{\beta}_{eq,single}} = N^{-\beta/2+1}$$

For $N=4$: $\dfrac{M_{multi}}{M_{eq,single}} = 0.62$

# Multi-rotor wind turbines 2000-

Ransom et. al, 2007-2010

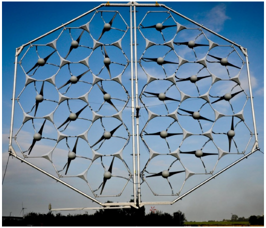

MOWIAN, 2012

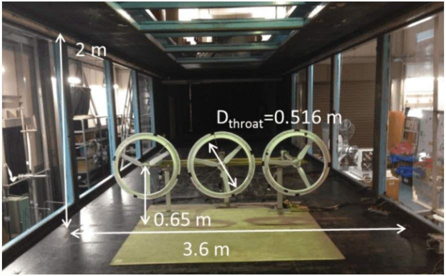


Kyushu University wind tunnel, 2014-2017

Kyushu University, 2014

# Approaches to fluid dynamics

- Hot wire anemometry
- Particle image velocimetry
- LIDAR

- Navier-Stokes equations have $\approx$ 80 exact solutions
- Engineering models

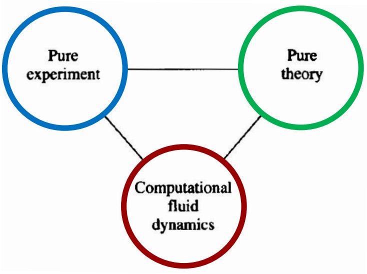


- Reynolds-Averaged Navier-Stokes (RANS)
- Large Eddy Simulations (LES)
- Direct Numerical Simulations (DNS)

# Computational methods

# Computational domain

| Cells pr. D | $N_x$ | $N_y$ | $N_z$ | Total Number of Cells |
|---|---|---|---|---|
| 5 | 128 | 96 | 64 | $\approx 0.79 \cdot 10^6$ |
| 10 | 224 | 128 | 96 | $\approx 2.8 \cdot 10^6$ |
| 20 | 384 | 192 | 128 | $\approx 9.4 \cdot 10^6$ |

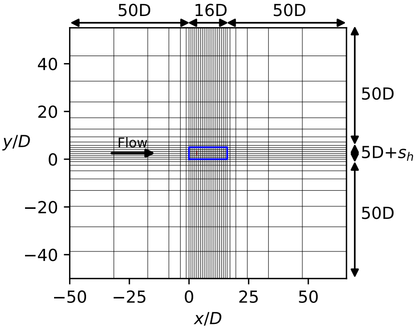


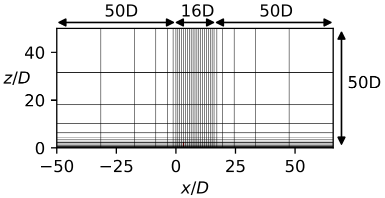

# Step 1: AD forces

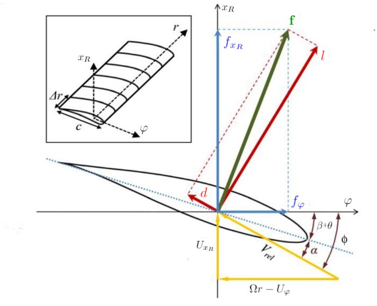


Forces are calculated using 2D airfoil data (aka. method III in van der Laan et. al (2015))

- **Calculation of AD forces**
- Redistribution of AD forces
- Flow solver

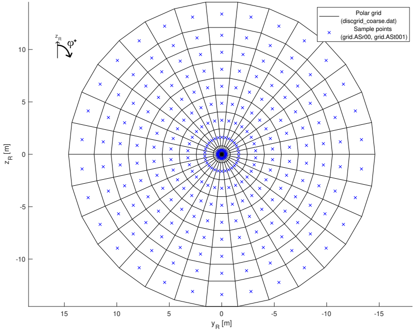


| AD grid | $N_\varphi$ | $N_r$ | $N_{AD}$ |
|---|---|---|---|
| Coarse | 30 | 9 | 270 |
| Fine | 180 | 94 | 16,920 |

# Step 2: Redistribution of forces

- Transfer forces from polar grid to computational domain

- Calculation of AD forces
- Redistribution of AD forces
- Flow solver

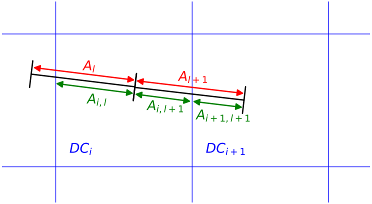


DC = Domain Cell

SC = Shape Cell

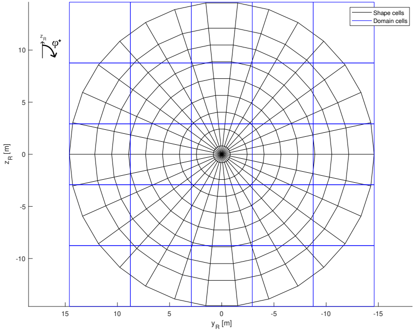

# Step 3: RANS equations

Assumptions:

- $\rho = 1.225 \frac{\text{kg}}{\text{m}^3}$
- $\mu = 1.784 \cdot 10^{-5} \frac{\text{kg}}{\text{m s}}$
- $\tau_{ij} = 2\mu S_{ij}$
- Inertial frame of reference

- Calculation of AD forces
- Redistribution of AD forces
- Flow solver

$$u_i = U_i + u_i' \quad , \quad p = P + p'$$

$$\overline{u_i' u_j'} = \frac{2}{3} k \delta_{ij} - \nu_T \left( \frac{\partial U_i}{\partial x_j} + \frac{\partial U_j}{\partial x_i} \right)$$

$$\boxed{\frac{\partial U_i}{\partial t} + U_j \frac{\partial U_i}{\partial x_j} = -\frac{1}{\rho}\frac{\partial P}{\partial x_i} + \frac{\partial}{\partial x_j}\left( (\nu + \nu_T)\frac{\partial U_i}{\partial x_j} - \frac{2}{3} k \delta_{ij} \right) + \frac{1}{\rho}\overline{f_i}}$$

6 variables:

$U, V, W, P, k, \varepsilon$

$$\boxed{\frac{Dk}{Dt} = \underbrace{\nabla \cdot \left( \left( \nu + \frac{\nu_T}{\sigma_k} \right) \nabla k \right)}_{\text{Diffusion}} + \underbrace{\mathcal{P}}_{\text{Production}} - \underbrace{\varepsilon}_{\text{Dissipation}}}$$

$$\boxed{\frac{D\varepsilon}{Dt} = \nabla \cdot \left( \left( \nu + \frac{\nu_T}{\sigma_\varepsilon} \right) \nabla \varepsilon \right) + (C_{\varepsilon,1}\mathcal{P} - C_{\varepsilon,2}\varepsilon)\frac{\varepsilon}{k}}$$

$$\boxed{\frac{\partial U_j}{\partial x_j} = 0}$$

# Neutral atmospheric boundary layer

$$U(z) = \frac{u_*}{\kappa} \log\left(\frac{z+z_0}{z_0}\right) \qquad k = \frac{u_*^2}{\sqrt{C_\mu}} \qquad \varepsilon = \frac{u_*^3}{\kappa(z+z_0)}$$

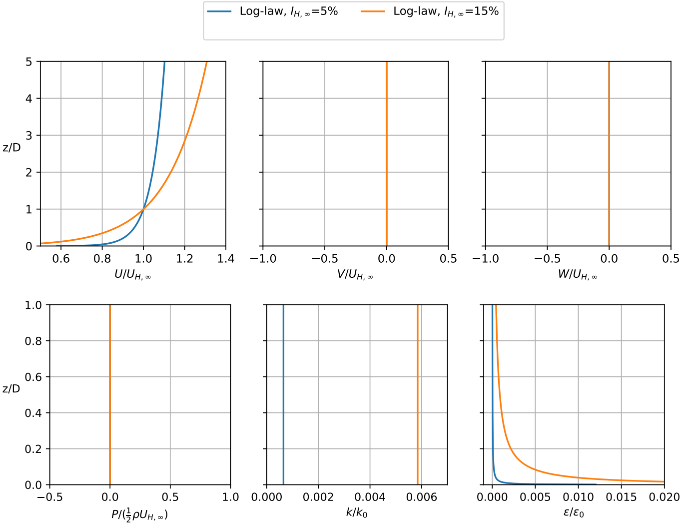

# Neutral atmospheric boundary layer

$$U(z) = \frac{u_*}{\kappa} \log\left(\frac{z+z_0}{z_0}\right) \qquad k = \frac{u_*^2}{\sqrt{C_\mu}} \qquad \varepsilon = \frac{u_*^3}{\kappa(z+z_0)}$$

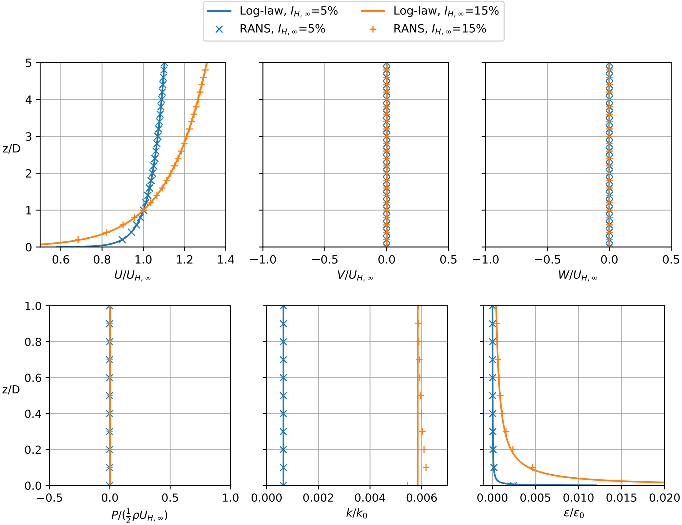

# Multi-rotor turbine studies

# Overview of studies

- Tip clearance
- Orientation of rotors
- Optimization of control
- Rotation
- Two aligned turbines

# Input parameters

- Focus on region 1, aka. "optimal $C_P$-tracking region"

| | |
|---|---|
| $z_H$ | $\{z_1, \frac{z_1+z_3}{2}\}$ |
| $U_{H,\infty}$ | 7 m/s |
| $I_{H,\infty}$ | $\{5, 15\}$ % |
| Computational grid | D/20 |
| AD grid | $N_\varphi = 64$, $N_r = 64$ |

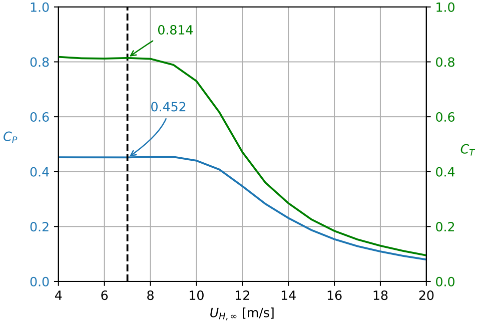

# Overview of studies

- Tip clearance
- Orientation of rotors
- Optimization of control
- Rotation
- Two aligned turbines

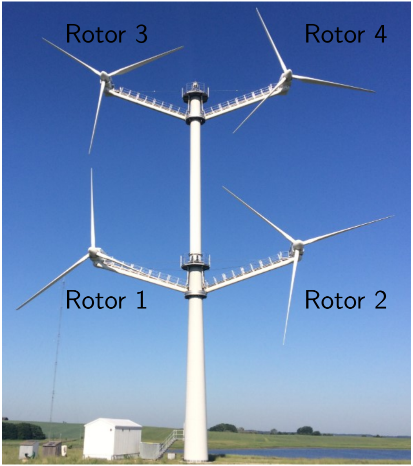

# Horizontal 2R-V29 - tip clearance 1/2

- Varying horizontal tip clearances: $s_h=\{0D,\ldots,4D\}$

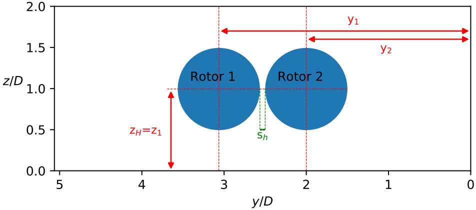


- Rotor interaction increases the power performance due to blockage effects, c.f. Smulders et. al (1984), Nishino and Draper (2015) and van der Laan et. al (2019)

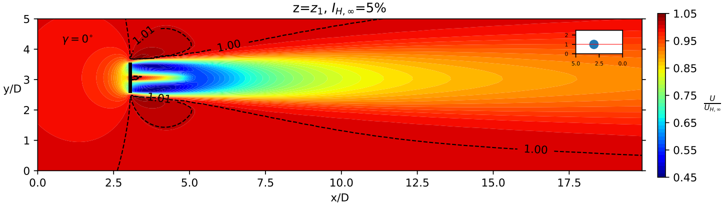

# Horizontal 2R-V29 - tip clearance 2/2

- Power of rotor 1 is compared to a freestanding single-rotor turbine
- Optimal tip clearance is $s_h/D \approx 0 - 0.15$ with resulting power increase of $0 - 1.8\%$ depending on $I_{H,\infty}$ and orientation

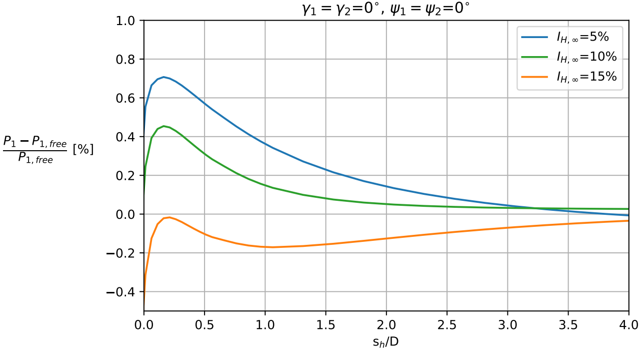

# Horizontal 2R-V29 - tip clearance 2/2

- Power of rotor 1 is compared to a freestanding single-rotor turbine
- Optimal tip clearance is $s_h/D \approx 0 - 0.15$ with resulting power increase of $0 - 1.8\%$ depending on $I_{H,\infty}$ and orientation

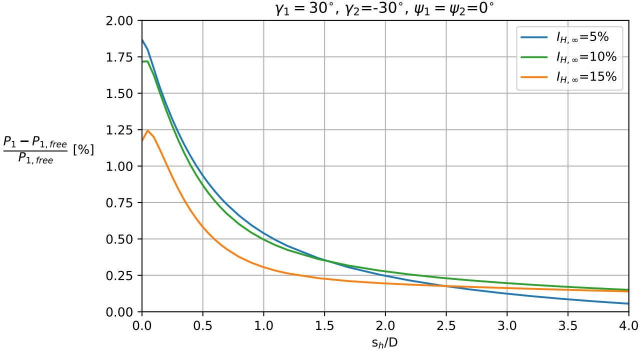

# Horizontal 2R-V29 - tip clearance 2/2

- Power of rotor 1 is compared to a freestanding single-rotor turbine
- Optimal tip clearance is $s_h/D \approx 0 - 0.15$ with resulting power increase of $0 - 1.8\%$ depending on $I_{H,\infty}$ and orientation

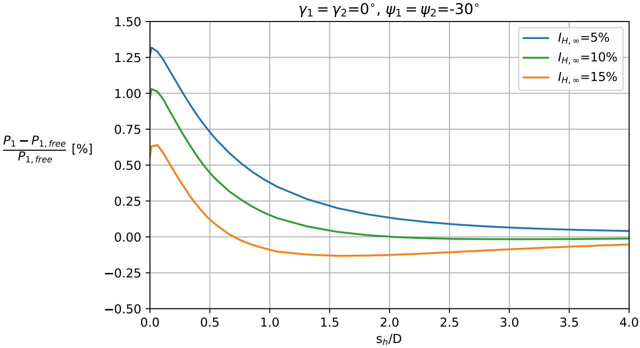

# Vertical 2R-V29 - tip clearance

- Power of rotor 1 is compared to a freestanding single-rotor turbine
- Power increase of $1.5 - 2.4\%$, but with largest increase for high $I_{H,\infty}$

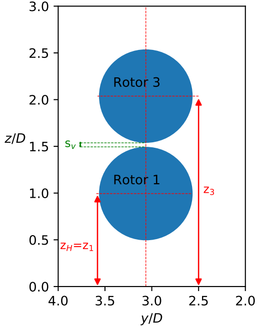


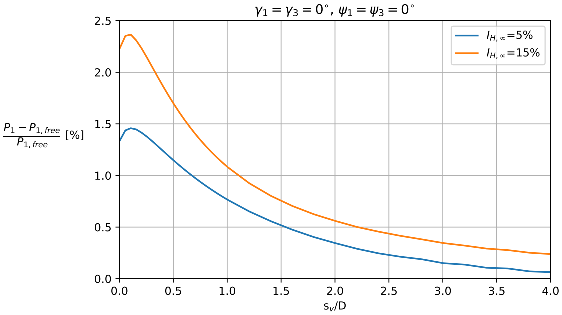

# Overview of studies

- Tip clearance
- **Orientation of rotors**
- Optimization of control
- Rotation
- Two aligned turbines

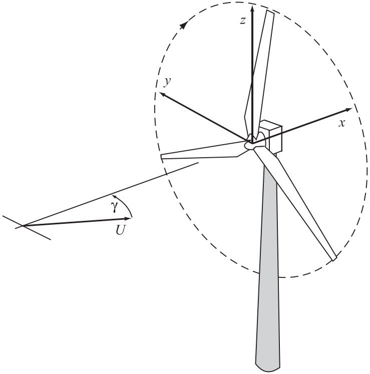

# Yaw of a single-rotor turbine 1/3

- Rotor 1 is yawed with $\gamma = \{0, 5, \ldots, 30\}^\circ$

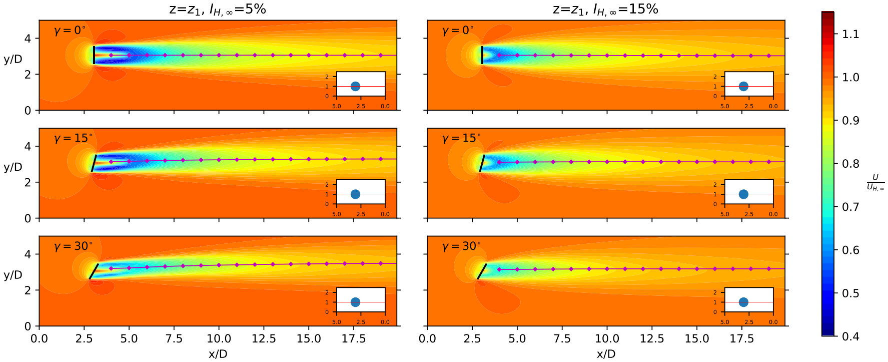

# Yaw of a single-rotor turbine 2/3

- Burton et al. (2001) derived from simple momentum considerations that $P \sim \cos^3(\gamma)$
- $P \sim \cos^2(\gamma)$ is used by for example ROMO Wind

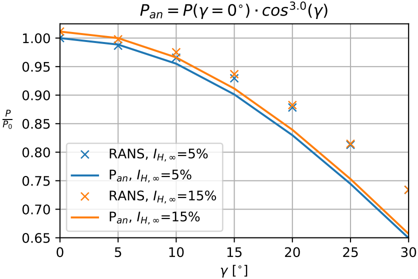


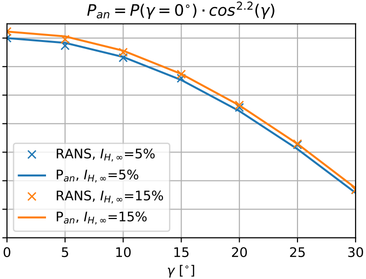

# Yaw of a single-rotor turbine 3/3

$$\frac{\int UdA}{\int U_0 dA} = \frac{\int_r \int_\varphi U(x,r,\varphi) rd\varphi dr}{\int_r \int_\varphi U(x/D{=}-42,r,\varphi) rd\varphi dr}$$

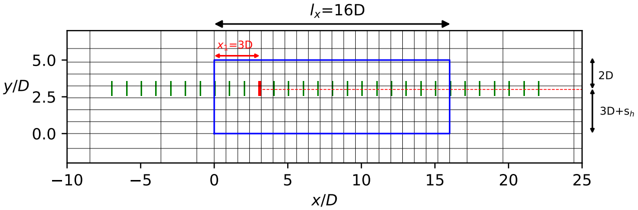


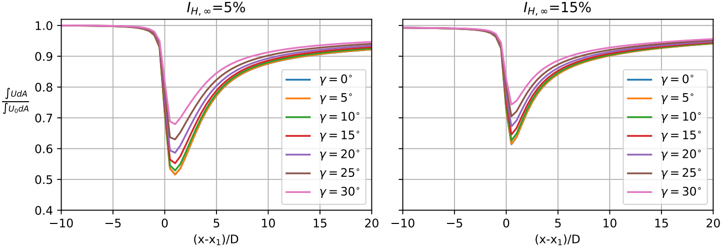

# Yaw of 4R-V29 support structures

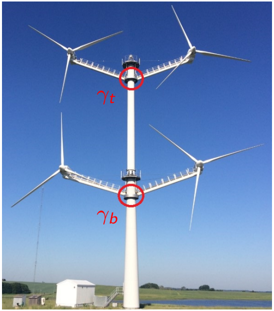


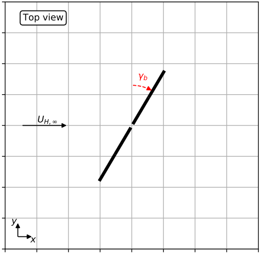


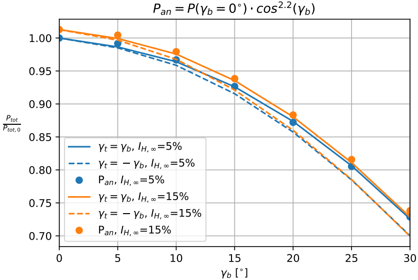


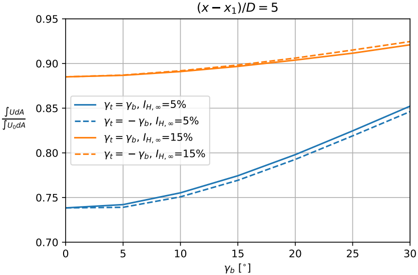

# 4R-V29 yaw and tilt

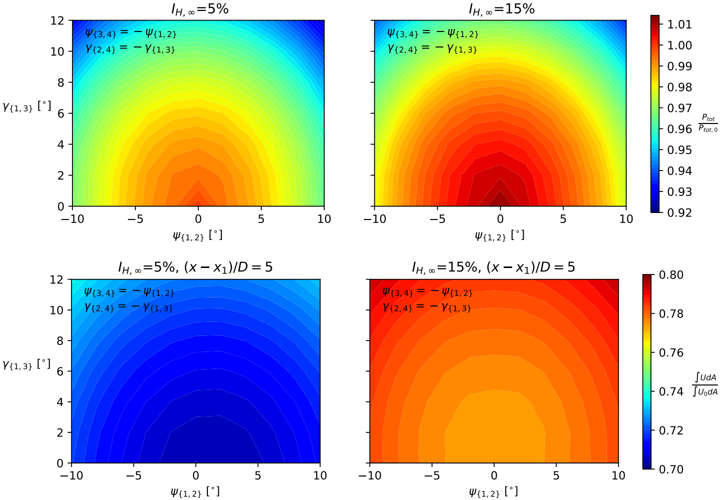

# Overview of studies

- Tip clearance
- Orientation of rotors
- **Optimization of control**
- Rotation
- Two aligned turbines

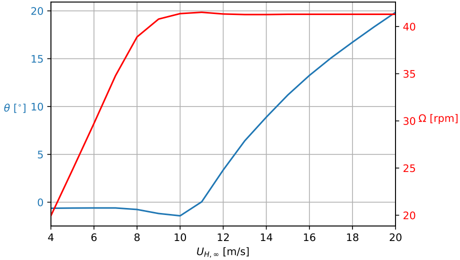

# V29 pitch-rpm optimization 1/3

- Buckingham-Pi theorem:

$$C_P = \frac{P(\rho,\mu,U_{H,\infty},R,\Omega,\theta_p)}{\frac{1}{2}\rho U_{H,\infty}^3 \pi R^2} = f(Re,\lambda,\theta_p) \approx f(\lambda,\theta_p)$$

- Python's derivative-free COBYLA optimizer is used with:

$$J(\theta,\Omega) = -P(\theta,\Omega)$$

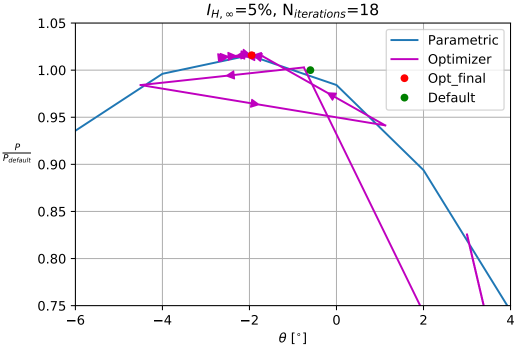

# V29 pitch-rpm optimization 2/3

- Parametric study: $\theta = \{-5, -4, \ldots, 1\}^\circ$ and $\Omega = \{33, 34, \ldots, 37\}$ rpm, which gives 35 combinations

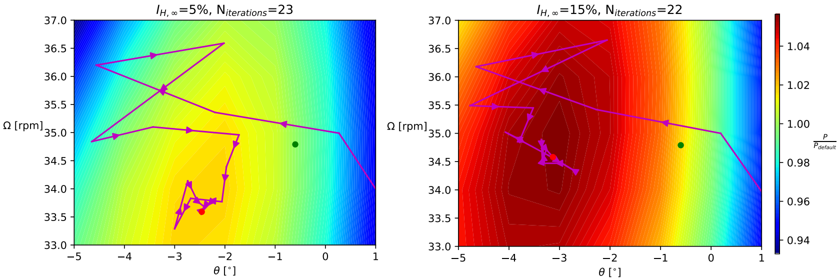


1. Vertically stretched grid
2. Induction zone and wake flow
3. Complex blade element aerodynamics

# V29 pitch-rpm optimization 3/3

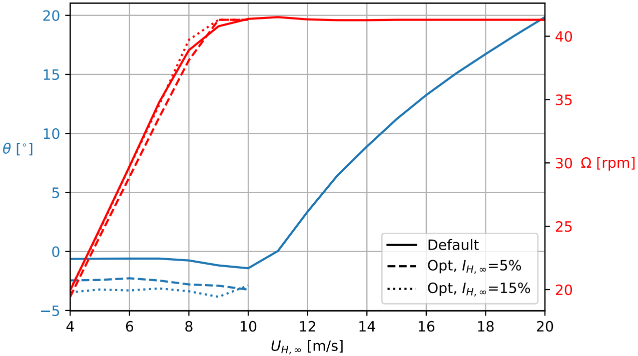


- Angle-of-attack buffer
- Default values tuned for noise
- Power increases of $1.8 - 3.8\%$

# 4R-V29 pitch-rpm optimization - 1/2

Two approaches for multi-rotor wind turbines:

- Individually optimized rotors:

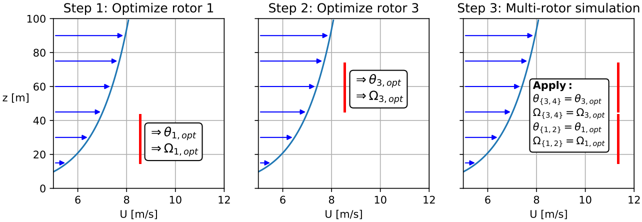


- Collectively optimized rotors: $(\theta_1, \Omega_1, \theta_2, \Omega_2, \theta_3, \Omega_3, \theta_4, \Omega_4)$ are used directly as design variables for the COBYLA optimizer

If rotor 1 and 2 operate equally, and rotor 3 and 4 operate equally:

$$(\theta_1, \Omega_1, \theta_2, \Omega_2, \theta_3, \Omega_3, \theta_4, \Omega_4) \rightarrow (\theta_1, \Omega_1, \theta_3, \Omega_3)$$

# 4R-V29 pitch-rpm optimization - 2/2

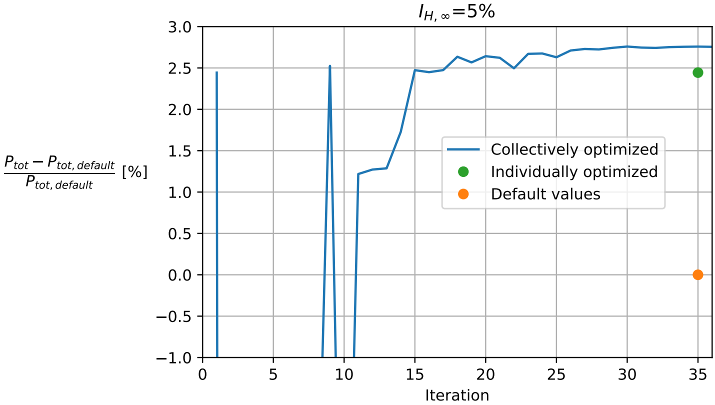


- Power increase of $\approx 5\%$ for $I_{H,\infty} = 15\%$

# Overview of studies

- Tip clearance
- Orientation of rotors
- Optimization of control
- **Rotation**
- Two aligned turbines

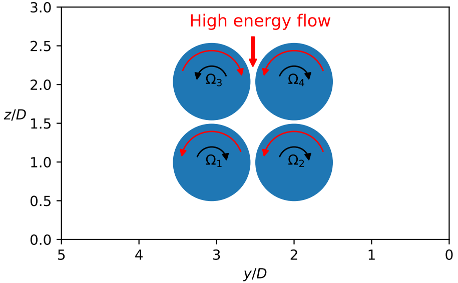

# 4R-V29 counter-rotating - 1/4

- Can counter-rotating rotors enhance wake recovery?
- Combination 4, 7, 9 and 12 seem promising, but almost no difference in power, thrust and wake recovery was observed

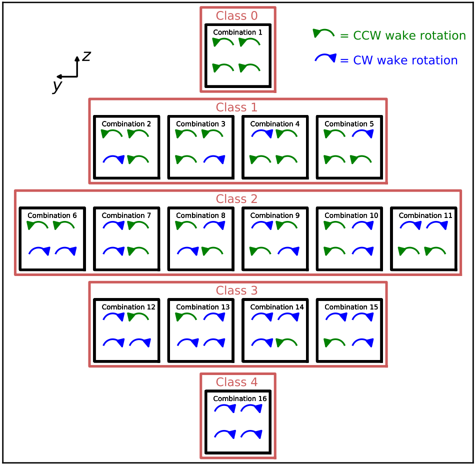

# 4R-V29 counter-rotating - 2/4

$$\varphi(y,z) = \text{atan2}\left(\frac{y_1 - y}{z - z_1}\right)$$

$$V_\varphi(y,z) = -V\cos(\varphi(y,z)) - W\sin(\varphi(y,z))$$

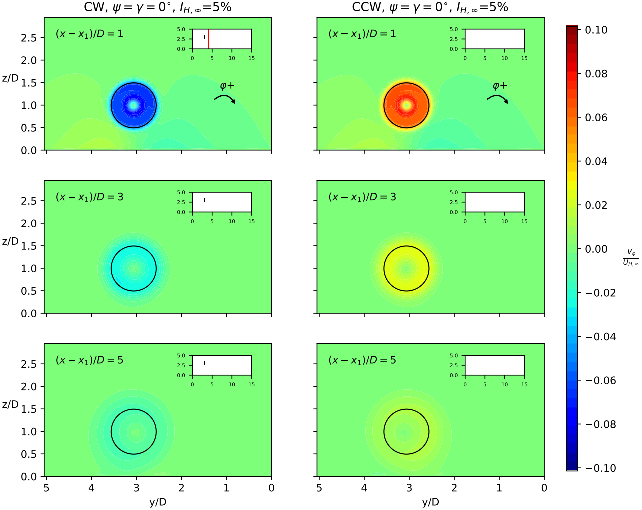

# 4R-V29 counter-rotating - 3/4

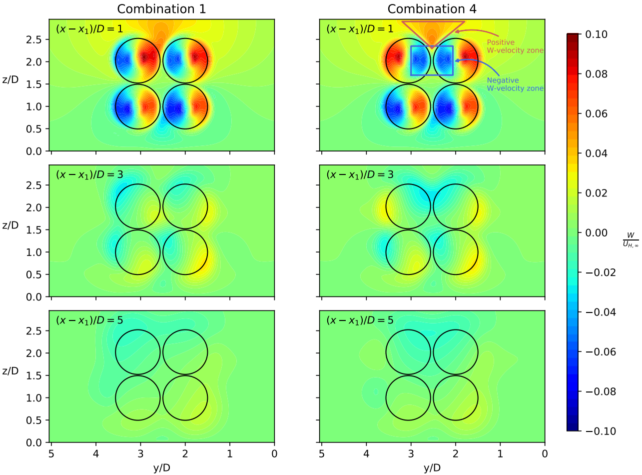

# 4R-V29 counter-rotating - 4/4

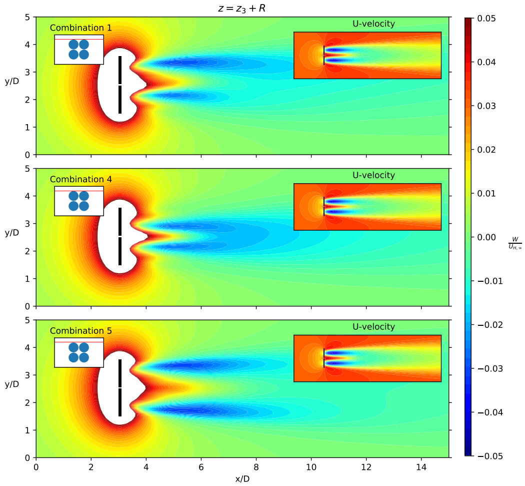


- Transient methods, e.g. URANS-AL or LES-AL, could yield other results

# Overview of studies

- Tip clearance
- Orientation of rotors
- Optimization of control
- Rotation
- **Two aligned turbines**

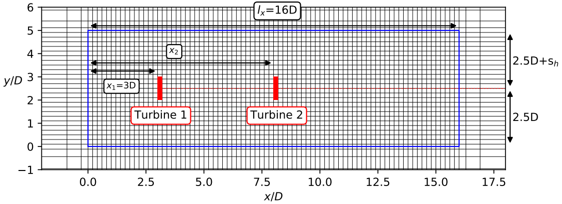


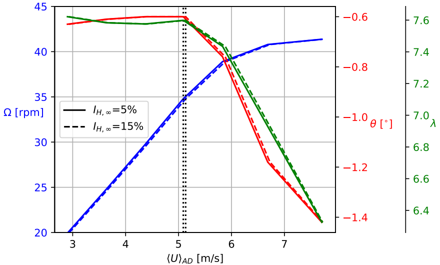


van der Laan et. al (2015)

# Two aligned 4R-V29 turbines

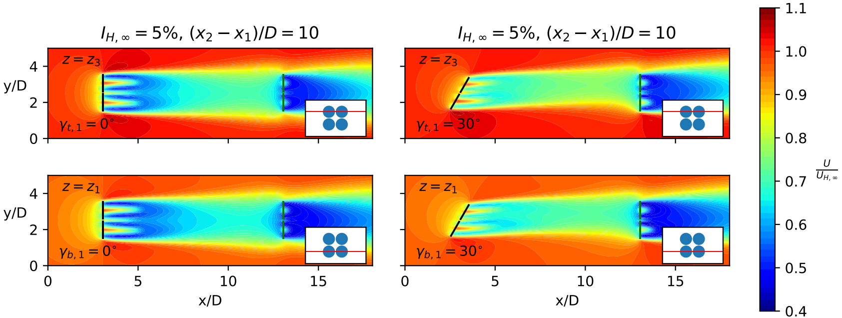


Turbine 1 could be de-regulated by adjusting:

- Yaw, i.e. $\gamma_b = \gamma_t$
- Rotational speed, i.e. $\Omega_{\{1,2\}}$ and $\Omega_{\{3,4\}}$

# Conclusion

# Conclusion

Summary of results:

- $P \sim \cos^{2.2}(\gamma)$ for both single- and multi-rotor turbines
- Pitch-rpm optimization improves power performance by 2-5%
- Effect of counter-rotating rotors is small
- Yaw steering does not improve power performance

Future work:

- Simulations with higher fidelity
- Comparison with equivalent single-rotor turbine
- Shutdown of rotors
- Staggered arrangements of rotors

# Thank you!

... questions?